SLAC/AP--48

DE86 009176

SLAC/AP - 48
February 1986
(AP)

OPTIMIZATION OF A LASERTRON DOUBLE OUTPUT CAVITY*

K. R. EPPLEY

Stanford Linear Accelerator Center
Stanford University, Stanford, California, 94305

ABSTRACT

Double output cavities have been used experimentally to increase the efficiency of high-power klystrons [1]. We have used particle-in-cell simulations with the 2+1/2 dimensional code MASK to optimize the design of double output cavities for the lasertron under development at SLAC. We discuss design considerations for double output cavities (e.g., optimum choice of voltages and phases, efficiency, wall interception, breakdown). We describe how one calculates the cavity impedance matrix from the gap voltages and phases. Some results of the effect of varying voltage, perveance, and pulse length are reported.

* Work supported by the Department of Energy, contract DE - AC03 - 76SF00515.

Introduction

Double output cavities have been used successfully in the 150 MW klystron to increase the output efficiency [1]. Herrmannsfeldt [2] has made preliminary calculations showing that a lasertron with two output cavities could have efficiencies approaching 70 percent. The aim of the present investigation was to optimize the cavity parameters for maximum efficiency and convert the simulation results into impedances from which the rf cavities could be designed and built.

Principles of Double Output Cavities

For typical high power microwave devices, a single output gap generally only extracts from 40-50% of the total energy. To extract the maximum energy from two gaps, the first gap should act as a combination output cavity and penultimate cavity. That is, it should have a low enough Q to extract some of the energy from the bunch, while having a fairly large inductive detuning so that some further bunching is done. The first gap extracts energy mainly from the front of the bunch while improving the bunching of the back of the bunch.

In principle there does not need to be a coupling between the two output cavities. One might connect each one to its own waveguide and adjust the path lengths so that the eventual recombination had the right phase. However, this presents problems of balancing the rf power when it is finally combined, and in practice it is simpler to couple the cavities through a slot and take the power out through a single waveguide. The slot introduces a coupling term to the impedance matrix:

$$\begin{pmatrix} V_1 \\ V_2 \end{pmatrix} = \begin{pmatrix} Z_{11} & Z_{12} \\ Z_{12} & Z_{22} \end{pmatrix} \begin{pmatrix} I_1 \\ I_2 \end{pmatrix} \qquad (1)$$

The klystron simulations were done using the particle-in-cell code MASK, described in [3]. The MASK code does not use the impedance matrix directly, but rather imposes the cavity voltage and phase as a boundary condition. From the results of the simulation one calculates the induced rf current as described by Yu [4]. Given the impedance matrix, it is possible in principle to solve iteratively from the MASK calculations to get voltages and phases for the cavities which satisfy (1). However, it is not trivial to find an algorithm which converges (except in the special case of all impedances identical, in which case both voltages and phases are equal). It is generally simpler to optimize the efficiency by adjusting each voltage and phase independently and then solve for the impedance matrix elements which satisfy (1). This system of equations appears to be underdetermined, since there are two equations and three unknowns. However, Zhao [5] has derived relations between the diagonal and off-diagonal terms in the impedance matrix for a coupled double output cavity:

$$
\begin{aligned}
&Z_{ij} \equiv \rho_{ij} + i\,\chi_{ij} \\
&\rho_{12} = \pm\sqrt{\rho_{11}\,\rho_{22}} \\
&\chi_{12} = \rho_{12}\left[\pm\left(\left(\frac{\chi_{11}}{\rho_{11}} + \cot\theta_{ss}\right)\left(\frac{\chi_{22}}{\rho_{22}} + \cot\theta_{ss}\right)\right)^{1/2} - \cot\theta_{ss}\right]
\end{aligned}
\tag{2}
$$

(θ_{ss} is the phase shift with the origin when both gaps are shorted.) If we assume that the second cavity is tuned near resonance we can take the $\cot\theta_{ss}$ term to be zero. Then:

$$
\chi_{12} = \pm\left(\chi_{11}\,\chi_{22}\right)^{1/2} \quad . \tag{3}
$$

These conditions, combined with the two voltages and two currents, completely define the impedance matrix.

Given voltages and currents from the MASK simulations, it is still not simple to solve this system of equations analytically. However, an iterative solution is straightforward, using Newton's method. (This solution requires negligible computer time. Since one can only obtain the currents for given voltages and phases by performing time-consuming MASK runs, it would be much more costly if one tried to solve the equations in the other way, i.e. to solve for voltages and phases given an impedance matrix.)

We note that there are two square roots in Eq. (2) which can have positive or negative signs. For the real part of the impedance we have taken the positive sign, since cavities with no sources of power should physically have positive real impedance. The sign for the imaginary term is not specified. We have found in general that the solution only converges for one choice of sign, depending on the signs of the diagonal terms. (We have no proof that a solution always exists, but as yet we have always been able to find one.)

Having solved for the impedance matrix, one must check that the coupled cavity system is stable. The stability criterion is that the magnitude of the beam conductance (which will have a negative maximum at the point of maximum power) must be less than the circuit conductance between the cavities. This condition must be met for the three modes of the coupled cavity system, and in general cannot be calculated until a specific cavity design is made. However, past experience with the 150 MW klystron indicates that stable cavities can be designed. (The cavity oscillation is an example of a feedback oscillator, where a voltage on cavity 1 induces a change in the beam current at cavity 2 which in turn causes a change in the voltage on cavity 1 after some time delay. If there is a positive feedback large enough to overcome the dissipation in the cavities the

system can oscillate.)

Once one has values for the impedance matrix one can then attempt to design a set of coupled cavities which matches the desired values. For a two pi mode the frequencies of the cavities should be close to resonance (2856 MHz at SLAC). Generally the cavities are designed approximately using codes such as LALA or SUPERFISH. Two dimensional codes can not include the effect of the output waveguide or the coupling slots. The presence of the waveguide can lower the frequency by a hundred megaherz or more, and the cavity designer takes this into account when designing the cavities. The shape and separation of the noses must be designed carefully, for they have a strong effect on the maximum field gradients and on the impedances.

Once a preliminary design is made, the cavity designer tests it using the method given by Zhao [5]. The impedance can be varied by adjusting the size of the waveguide iris, the gap widths, and the orientation of the coupling slots. By trial and error one can construct an impedance matrix which is a good approximation to the desired one.

Design Constraints

There are a number of factors which must be considered in a realistic cavity design. First, the gap sizes must be large enough to withstand the voltage without breakdown or multipactor. A rough rule of thumb is that the maximum electric fields on the walls of the cavity should be no more than about 300 kV/cm at the operating frequency. Calculations with codes such as LALA and SUPERFISH usually show maximum field strengths about 1.5-1.6 times higher than the average field across the gap. (However, the 300 kV/cm criterion may be conservative.

The 5045 klystron, which was designed for 315 kV using this criterion, has been run at 350-400 kV without serious breakdown problems.) Once a preliminary design is made, a more precise determination can be done using multipactor codes. Subject to this constraint, one wishes to make the gaps as narrow as possible to improve coupling and hence efficiency.

Similarly, the tube diameter must be large enough to prevent significant interception before the final output cavity, as this wastes beam energy and will damage the walls. A rule of thumb is that one should make the tube diameter about 30 per cent larger than the beam size at input. (Since MASK can calculate radial dynamics more accurately than the one dimensional codes previously used for design, we may be able to allow a smaller margin.) A certain amount of interception is permissible after the output cavities, but if this is too high damage to the walls will occur. A rule of thumb is to allow no more than about 500 watts/cm^2 average power absorbed for copper walls. For the walls between the two output cavities the requirements are more stringent because the presence of the coupling slot impedes the heat transfer from the walls to the outside. Interception in this section of the tube should amount to no more than about 2 kW average power. One wishes to make the tube diameter as small as possible, consistent with these constraints, to improve the coupling with the beam and thus improve the efficiency.

There is also a constraint on the separation between the two coupled output cavities. For the mode of operation (pi or two pi, etc.), there is a natural distance between cavities, depending on the beam velocity and the phase shift between the voltage and current, which will give maximum power out. However, the separation between the gaps cannot be too large, or else it will be difficult to

couple power through a slot to the second cavity. In practice, the slot should not be much longer than about a centimeter. In the case of the 150 MW tube, the cavities were made long and narrow so that they shared a common wall, while allowing the gaps to be about 6 cm apart. However, separations much longer than this would be difficult. The 150 MW tube used a two pi mode. The reason this was chosen rather than a pi mode was that experience had shown that for the pi mode there was a net flow of current between the cavities, resulting in a deflection of the beam. However, the cavities studied with pi modes had a single coupling slot, and it is possible that the deflection could be prevented by using a pair of slots.

Optimization of the Lasertron Cavities

As a starting point, we began with the lasertron geometry designed by Welch [6] for a single output cavity. This established the shape and position of the cathode and anode and the drift tube. We used the same pulse shape, which was a trapezoid with a linear ramp-up for 43.8 ps, a flat top for 13.7 ps, and a linear ramp-down for 43.8 ps. (This approximates a Gaussian with FWHM of about 60 ps.) The average current over the entire rf period was 124 amperes, with beam voltage of 400 kV, for a microperveance of .49. With a single cavity we obtained a maximum efficiency of about 63 per cent, in reasonable agreement with Welch's findings. This is higher than that of the 50 MW klystron because the lasertron has better bunching and lower perveance.

To model the second cavity we made some minor changes in the original design. A longer solenoid was assumed than that planned for the single cavity (15.3 cm long instead of 10.3 cm). We used slightly narrower gaps (16 mm)

because the voltage for the two gap system will be lower on each gap. The 16 mm value is similar to the size of a klystron output cavity designed to operate with 300-350 kV volts at 2856 MHz, and within the 300 kV/cm estimate.

The cavity parameters and geometry were optimized for maximum efficiency with a two pi mode (allowing about 15 degrees phase difference between the gap voltages). The magnitude of the voltages were taken to be approximately equal, in accordance with the results of the 150 MW klystron, and small variations of the voltages indicated that this was near the optimum. The optimal phase differences between gap voltages and currents were found to be about .7 radians (inductive) for gap 1 and .1 radians (capacitative) for gap 2. The optimum voltages for the 400kV beam were about 295 kV across the gaps. For the two pi mode, the optimal separation between gap centers was 68 mm. The efficiency was improved by reducing the tube diameter to 14 mm at the first gap, where the beam is most focused by the magnetic field. The beam expands afterwards and the tube was expanded to 15 mm beginning at 20 mm after the end of the first gap. (See Figure 1.) To improve clearance, the anode mouth was kept at a radius of 18 mm until within 8 mm of the first gap. The coil current was also increased slightly to 50000 ampere turns (peak field of 1790 gauss). With these adjustments the efficiency was calculated to be 76.5 per cent. The efficiency as calculated by the rf E·J agreed to that from kinetic energy change to within two per cent, indicating good energy conservation in the calculation.

The voltages and currents for the optimum values were found to be:

$$V_1 = 2.95 \times 10^5 \ \exp(-.098i)$$

$$V_2 = 2.96 \times 10^5 \ \exp(-.356i)$$

$$I_1 = 172 \ \exp(-.807i) \tag{4}$$

$$I_2 = 126 \ \exp(-.242i) \quad .$$

Imposing the Zhao condition given above, we solved numerically for the impedance matrix and obtained:

$$Z_{11} = 1012 \ \exp(.619i)$$

$$Z_{22} = 1057 \ \exp(.108i) \tag{5}$$

$$Z_{12} = 966 \ \exp(.272i) \quad .$$

Note that the MASK convention defines voltages and phases, and hence impedances, at the cavity gap. If one wishes to convert to impedances defined in terms of voltages on axis, one must scale the voltages by the ratio of voltages on axis to voltages at the gaps. The impedances will scale as the square of this ratio. In the case of variable radius this factor will differ between the two cavities. Then the diagonal elements scale as the square of the voltage ratio for the corresponding cavity, while the cross term scales as the product of the ratio. That is:

$$r \equiv V_{\text{wall}}/V_{\text{axis}}$$

$$Z_{11}(\text{axis}) = Z_{11}(\text{wall})/r_1^2$$

$$Z_{22}(\text{axis}) = Z_{22}(\text{wall})/r_2^2 \tag{6}$$

$$Z_{12}(\text{axis}) = Z_{12}(\text{wall})/(r_1 \, r_2) \quad .$$

For the tube radii we used (14 mm for gap 1 and 15 mm for gap 2) the voltage ratios can be calculated (expanding the cylindrical Bessel function solution across the gap):

$$r_1 = .855$$

$$r_2 = .833 \quad . \tag{7}$$

Thus the axis impedances will be as follows:

$$Z_{11} = 1384 \ \exp(.619i)$$

$$Z_{22} = 1523 \ \exp(.108i) \tag{8}$$

$$Z_{12} = 1356 \ \exp(.272i) \quad .$$

Construction of the Actual Cavity System

A double output cavity based on the design above was built by Terry Lee. The dimensions are shown in Figure 8. It was not possible to match the computer optimized values exactly. The best approximation achievable in practice was measured to have the following (axis) impedences:

$$Z_{11} = 1310 \ \exp(.162i)$$

$$Z_{22} = 1760 \ \exp(.154i) \tag{9}$$

$$Z_{12} = 1517 \ \exp(.154i) \quad .$$

We were able to iterate the MASK runs by Newton's method to obtain a set of voltages and phases consistent with these impedences. The way we did this was by starting with an initial guess for the solution and calculating the

corresponding impedences as described above. Then we ran MASK calculations with a small change in the voltage on the first cavity and again for the second cavity. Assuming that the induced currents were analytic functions of the cavity voltages for small variations about the given solution, we calculated the partial derivatives of the currents with respect to the voltages and solved the simultaneous equations to obtain a next guess at the solution. This procedure converged after a few iterations to a reasonable agreement with the desired impedences. The calculated voltages and currents were:

$$\begin{aligned} V_1 &= 2.60 \times 10^5 \ \exp(-.408i) \\ V_2 &= 3.00 \times 10^5 \ \exp(-.413i) \\ I_1 &= 166 \ \exp(-1.008i) \\ I_2 &= 131 \ \exp(-.074i) \quad . \end{aligned} \tag{10}$$

This set of voltages and currents corresponds to the following impedence matrix:

$$\begin{aligned} Z_{11} &= 1322 \ \exp(.160i) \\ Z_{22} &= 1747 \ \exp(.150i) \\ Z_{12} &= 1520 \ \exp(.154i) \quad . \end{aligned} \tag{11}$$

The simulation predicted an efficiency of 73.6 per cent or about 3 points less than the optimized value.

Effect of Varying Voltage and Current

We have examined the effect on the rf power and efficiency of varying the perveance, pulse length, and voltage around the nominal design values. To vary the perveance, we used the same pulse shape and duration and changed the current intensity. To vary the pulse length, the current density was kept constant and the ramp-up, peak, and ramp-down times were scaled by a constant factor. Thus this also corresponds to a variation in perveance. To vary the voltage, we kept the same pulse length and scaled the current to get a particular perveance.

These variations do not keep the impedance matrix constant. This represents an approximate optimization for each case, because the gap separations and tube radii were not varied. When the beam voltage was varied, the gap voltage and the gap widths were scaled linearly with beam voltage. If perveance is varied by a constant factor, with constant voltage, cavity impedance should be changed by the same factor.

The results are displayed in Figures 3-6. We found that small variations in perveance or pulse length did not result in large losses in efficiency. Rf power continued to increase with increasing perveance until about microperveance 1., at which point it began to fall, with a large decrease in efficiency. This was true whether perveance was increased by increasing the pulse length or the peak current. However, for the same perveance, shorter pulses gave somewhat higher efficiency. Efficiency showed a slight increase with voltage. (We note that not as much time was spent in optimizing these runs as was spent on the nominal case. Thus the true optimum values may lie one or two points higher than shown. However, general trends are probably valid.)

We found that one can get considerably more power from the lasertron by increasing the perveance if a somewhat lower efficiency is acceptable. If the tube could be redesigned to withstand higher voltages, this would also produce higher power. If large variations in current or voltage are contemplated for the lasertron test, optimal efficiency will probably be attainable only if it is possible to vary the cavity impedance, e.g., with an external EH tuner, internally tunable cavities, or both. (That is, changing the perveance with the same cavity impedance would change the cavity voltages to a value which in general would produce lower efficiency.)

Conclusions

We have found an increase in power of about 20 percent from a double output cavity compared to the maximum obtainable with a single cavity. The performance is not sensitive to small (order 10 percent) changes in pulse length, perveance, or voltage. Maximum output power is achieved at about 1. microperv, at a somewhat lower efficiency than at the design value.

References

1. T. G. Lee, G. T. Konrad, Y. Okazaki, M. Watanabe and H. Yonezawa, "The Design and Performance of a 150 MW Klystron at S-Band," SLAC-PUB-3619, April 1985.

2. W. B. Herrmannsfelt, "Lasertron Simulation with a Two-Gap Output Cavity," SLAC/AP-41, April 1985.

3. A. Palevsky and A. T. Drobot, "Application of E-M P.I.C. Codes to Microwave Devices" in Proceedings, Ninth Conference on Numerical Simulation of Plasmas, paper PA-2, Northwestern University, Evanston, Illinois, June 30-July 2, 1980.

4. S. Yu, "Particle-In-Cell Simulation of High Power Klystrons," SLAC/AP-34, September 1984.

5. Y. Zhao, "An Impedence Measurement Method for Double-Gap Klystron Cavity," IEEE Transactions on Electron Devices, Vol. ED-29, No. 2, February 1982, pp. 316-320.

6. J. Welch, "Efficiency and the Lasertron," SLAC, September, 1985.

Figure Captions

Figure 1A. Geometry of the lasertron simulation. All dimensions in mm. (R and z scales are not the same.)

Figure 1B. Electron position-space distribution, 4.902 ns.

Figure 1C. Electron position-space distribution, 4.989 ns (plots are in 90 degree phase increments).

Figure 1D. Electron position-space distribution, 5.077 ns.

Figure 1E. Electron position-space distribution, 5.165 ns.

Figure 2A. Electron z-momentum versus z., 4.902 ns. (vertical axis is $\gamma \cdot v_z$).

Figure 2B. Electron z-momentum versus z, 4.989 ns.

Figure 2C. Electron z-momentum versus z, 5.077 ns.

Figure 2D. Electron z-momentum versus z, 5.165 ns.

Figure 3. Rf power versus DC input power for optimized values at various operating points.

Figure 4A. Rf power versus laser pulse length (FWHM), 400 kV. Gaussian shape was approximated by a trapezoid. 60 ps corresponds to perveance .5 μpervs.

Figure 4B. Efficiency versus laser pulse length, 400 kV.

Figure 5A. Rf power versus perveance, constant pulse length (60 ps), 400 kV.

Figure 5B. Efficiency versus perveance, constant pulse length, 400 kV.

Figure 6A. Rf power versus DC voltage, perveance .75 μpervs.

Figure 6B. Efficiency versus DC voltage, perveance .75 μpervs.

Figure 7. B_z magnetic field profile on axis, 50000 ampere turns.

Figure 8. Dimensions of double output cavity as actually built.

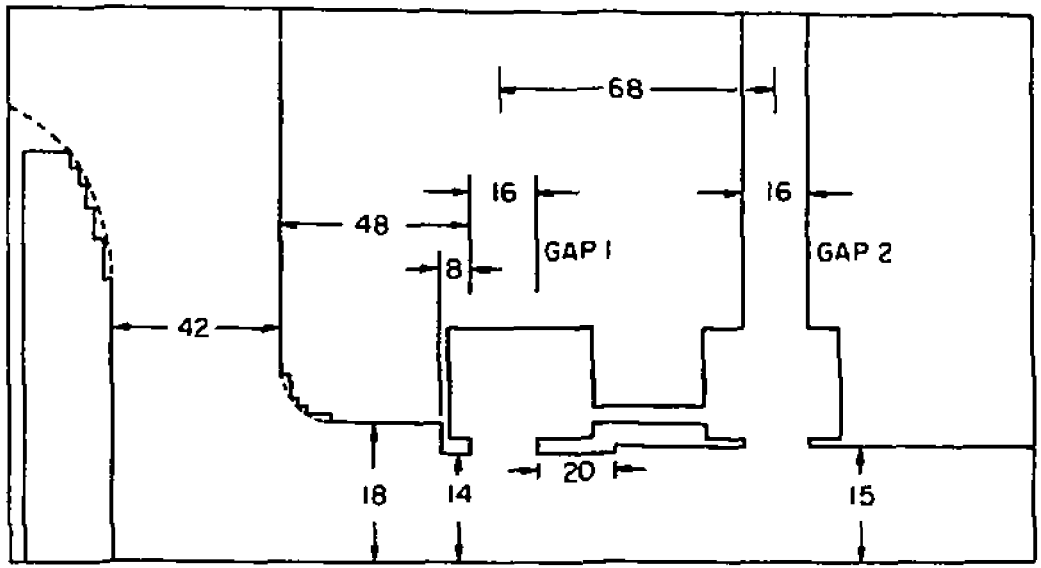

FIGURE 1A

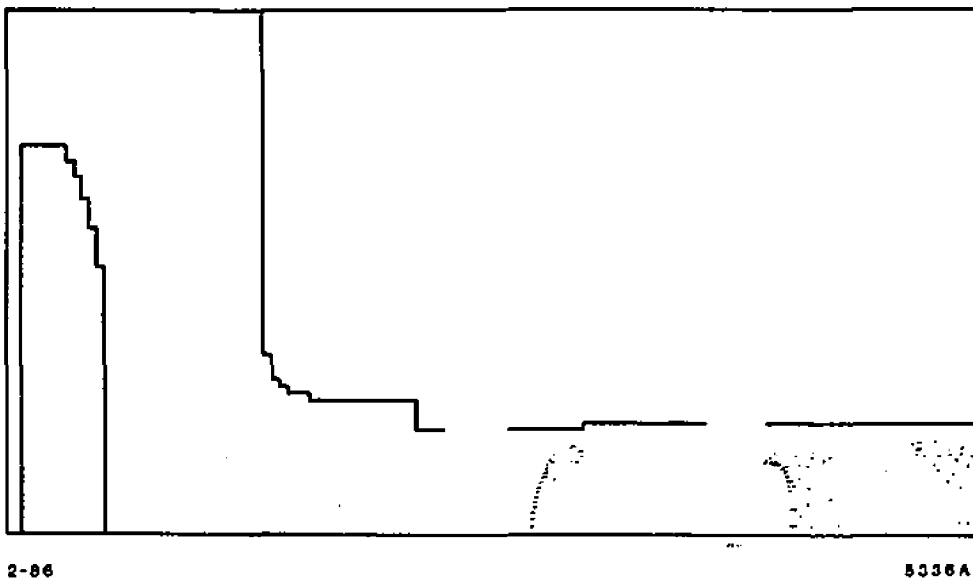

FIGURE 1B

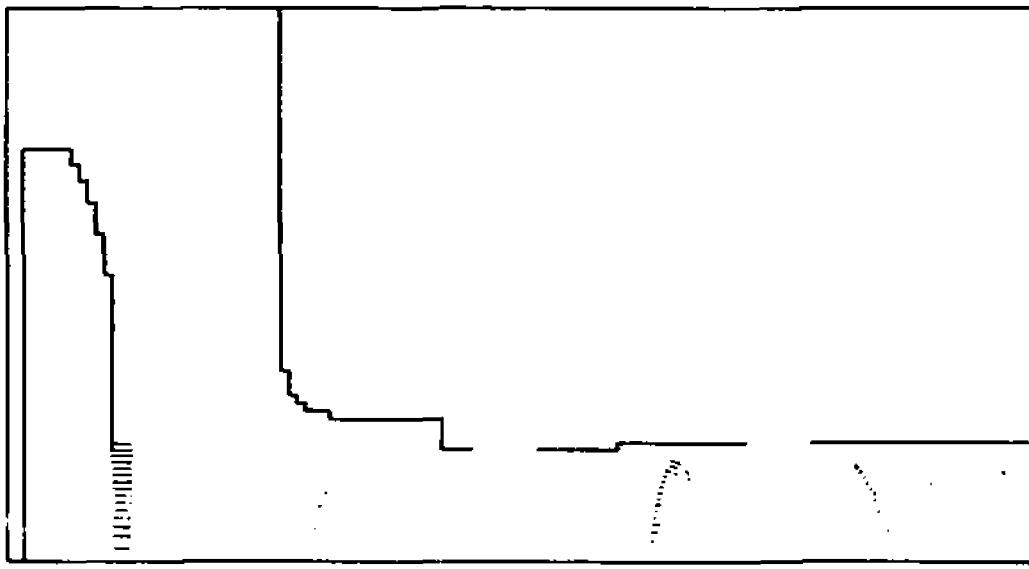

FIGURE 1C

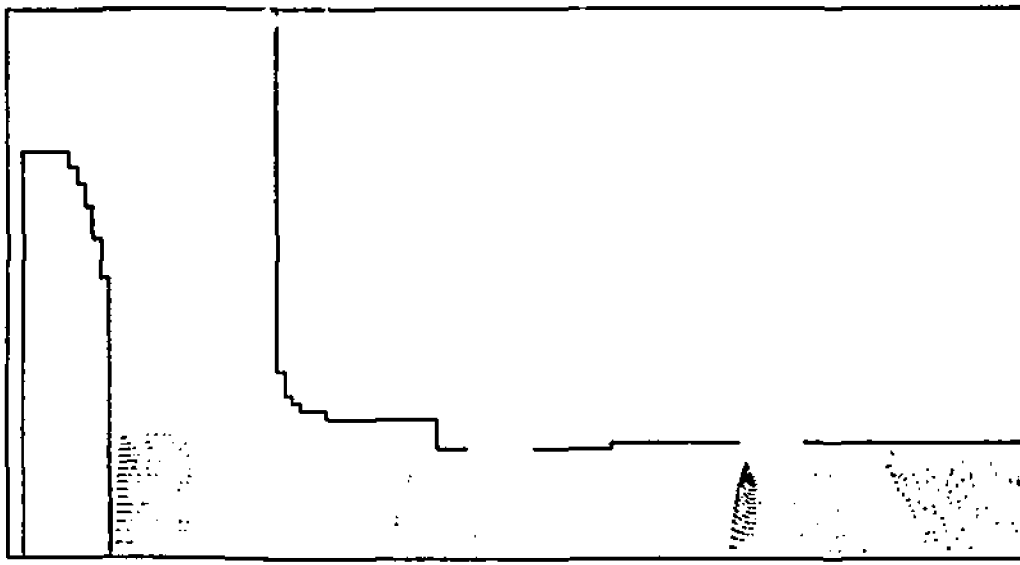

2-80

5336A4

FIGURE 1D

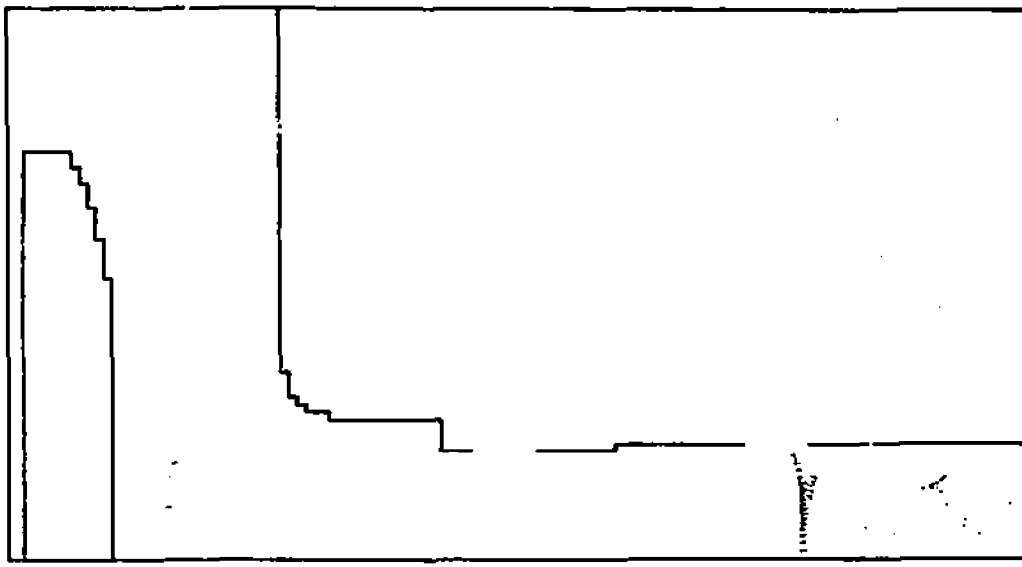

FIGURE 1E

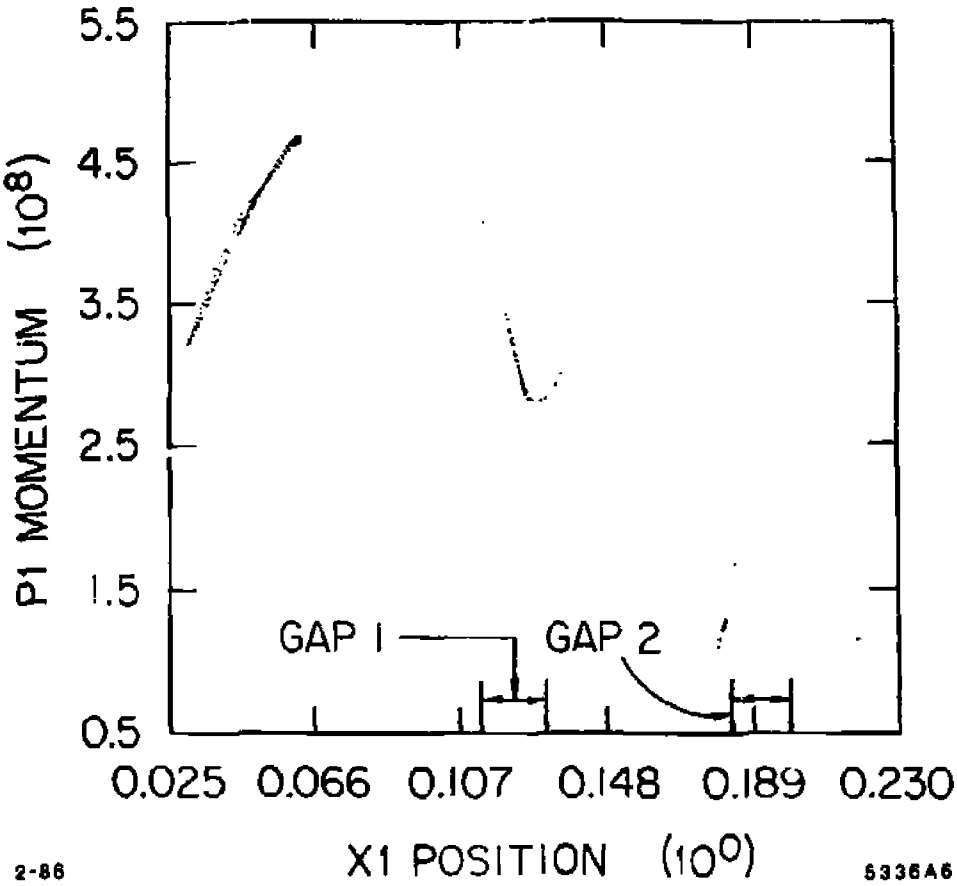
5.5
4.5
3.5
2.5
1.5
0.5
P1 MOMENTUM (10^8)
GAP 1
GAP 2
0.025 0.066 0.107 0.148 0.189 0.230
X1 POSITION (10^0)
2-86
5336A6

FIGURE 2A

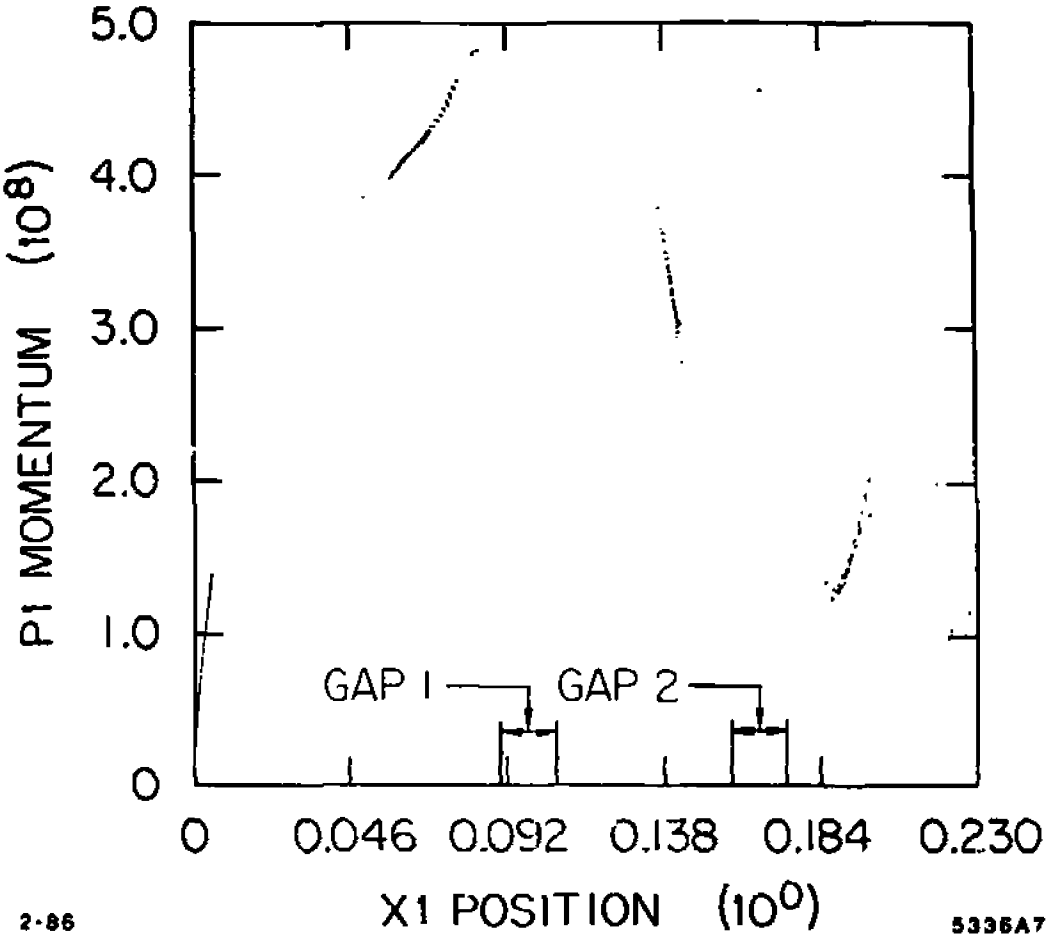
5.0
4.0
3.0
2.0
1.0
0
P1 MOMENTUM (10^8)
GAP 1
GAP 2
0
0.046
0.092
0.138
0.184
0.230
X1 POSITION (10^0)
2-86
5336A7

FIGURE 2b

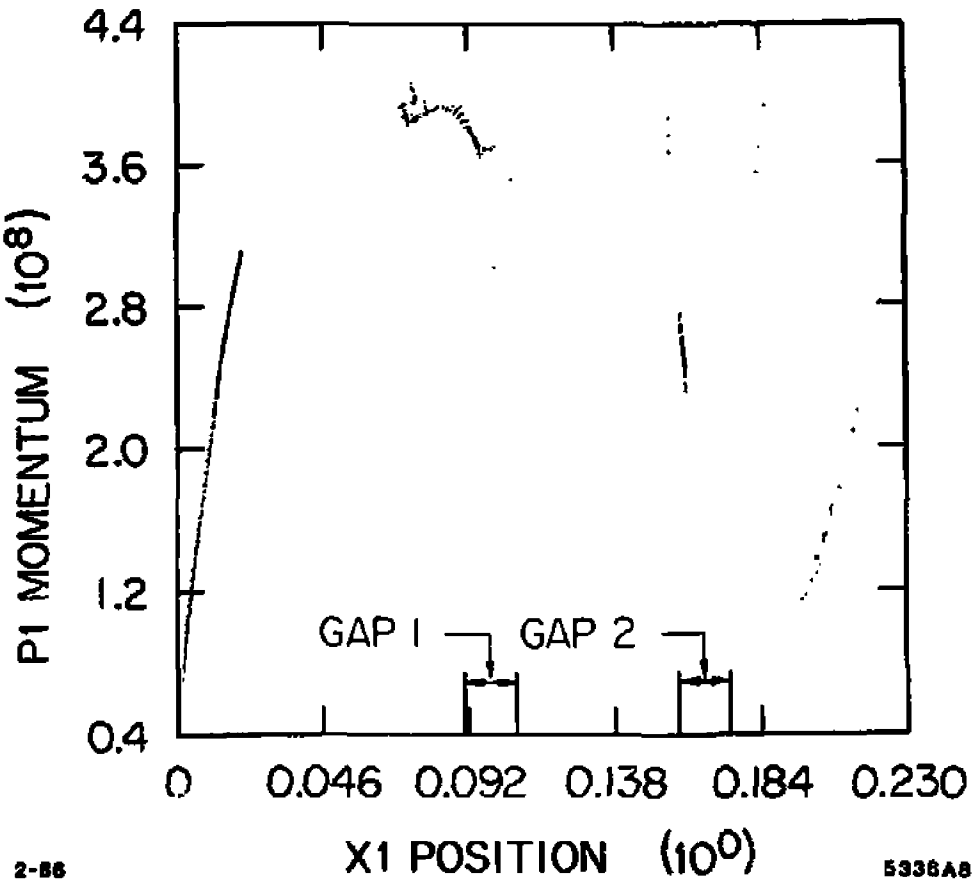
4.4
3.6
2.8
2.0
1.2
0.4
P1 MOMENTUM (10^8)
GAP 1
GAP 2
0
0.046
0.092
0.138
0.184
0.230
X1 POSITION (10^0)
2-86
5336A8

FIGURE 2C

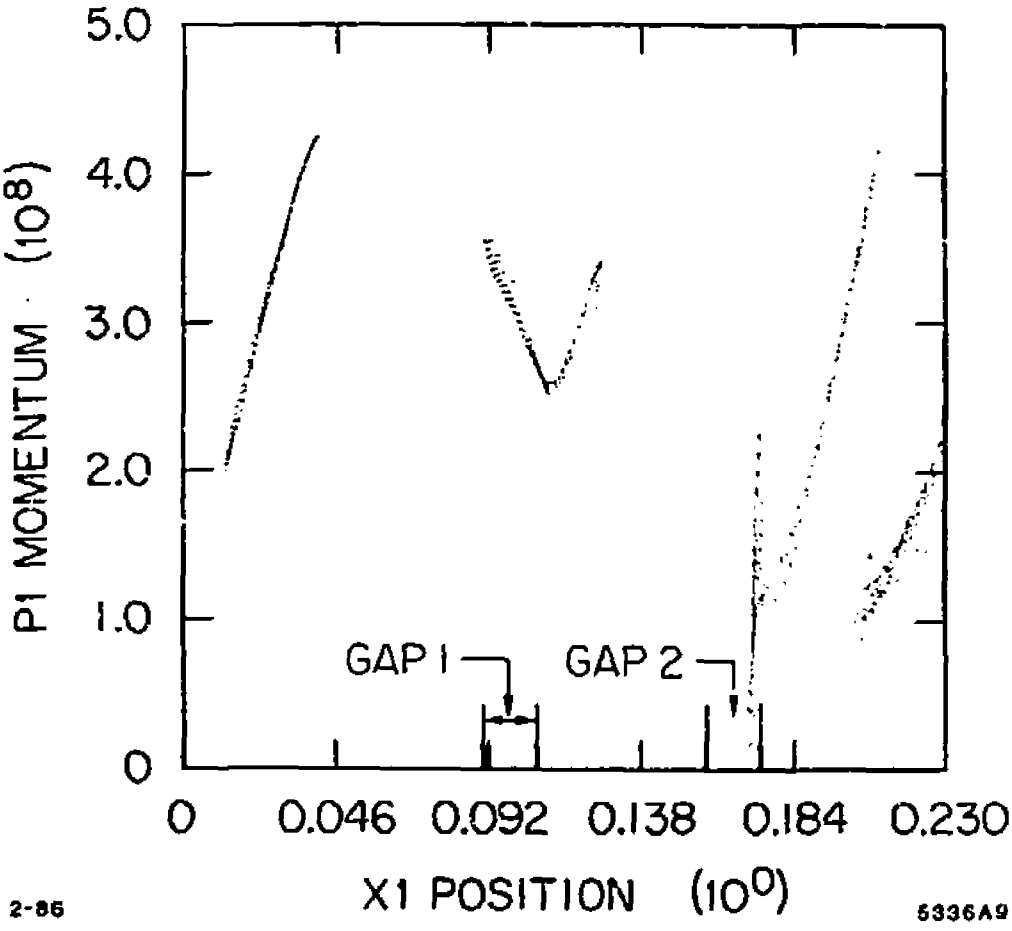
5.0
4.0
3.0
2.0
1.0
0
P1 MOMENTUM · (10^8)
GAP 1
GAP 2
0
0.046
0.092
0.138
0.184
0.230
X1 POSITION (10^0)
2-86
5336A9

FIGURE 2D

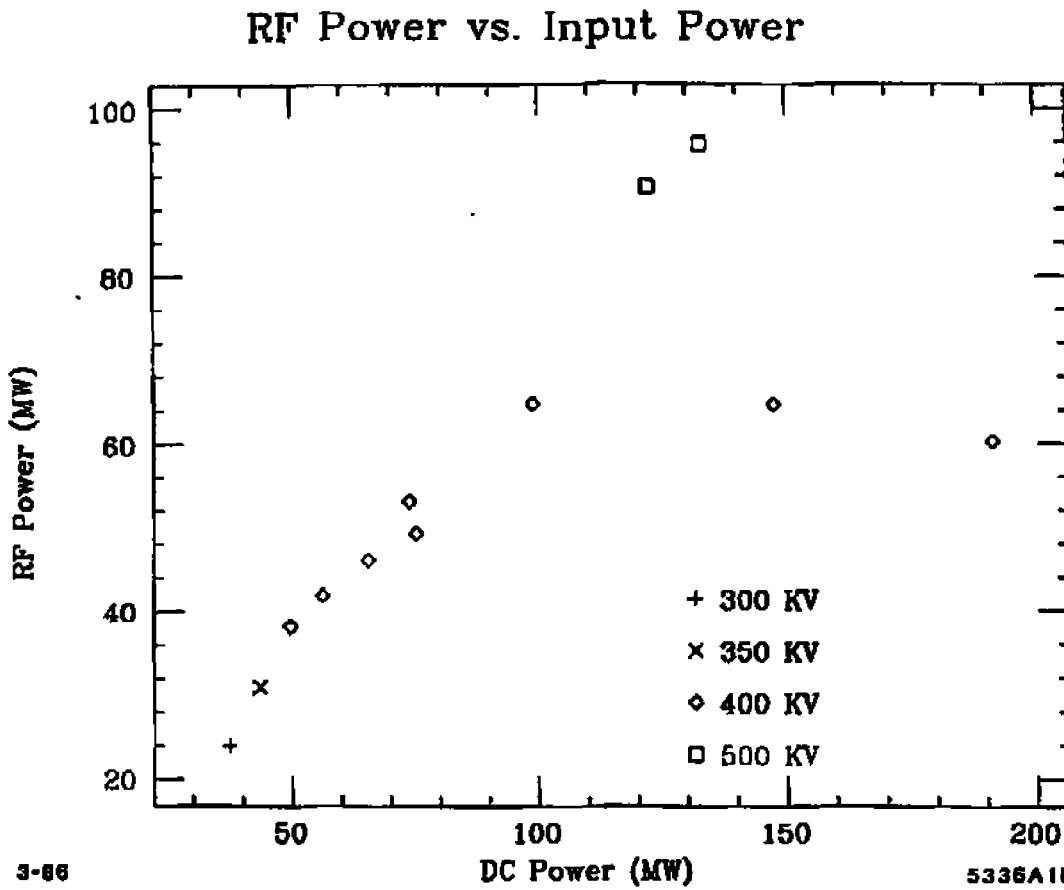
RF Power vs. Input Power
RF Power (MW)
100
80
60
40
20
50
100
150
200
DC Power (MW)
+ 300 KV
× 350 KV
◇ 400 KV
□ 500 KV
3-86
5336A18

FIGURE 3

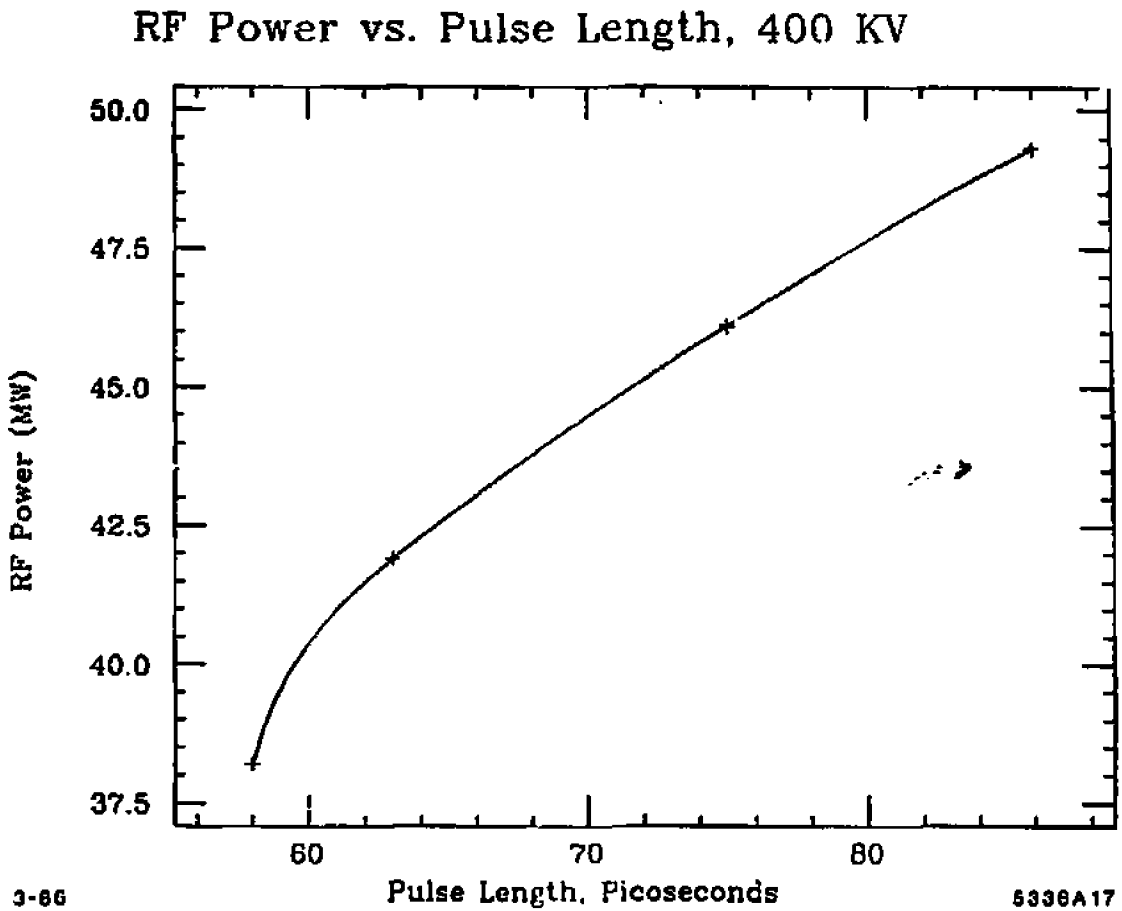
RF Power vs. Pulse Length, 400 KV
50.0
47.5
45.0
42.5
40.0
37.5
RF Power (MW)
60
70
80
Pulse Length, Picoseconds
3-86
5336A17

FIGURE 4A

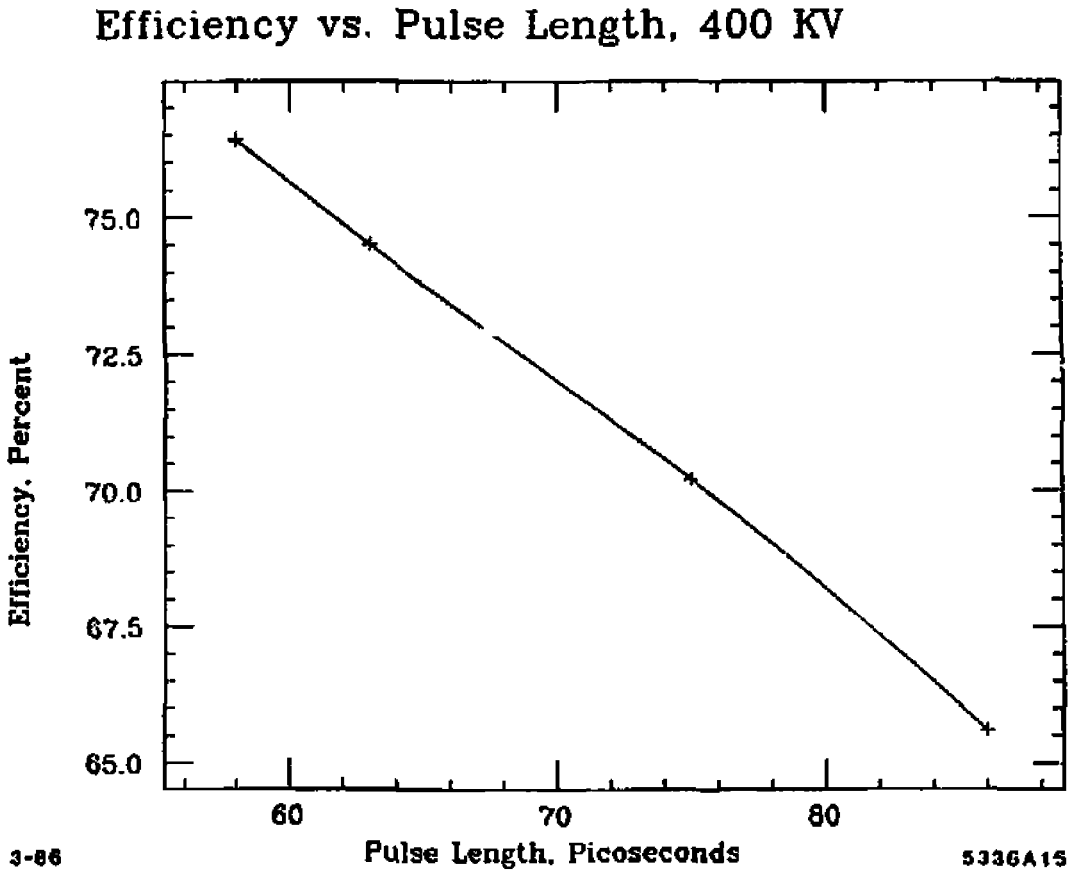
Efficiency vs. Pulse Length, 400 KV
75.0
72.5
70.0
67.5
65.0
Efficiency, Percent
60
70
80
Pulse Length, Picoseconds
3-86
5336A15

FIGURE 4B

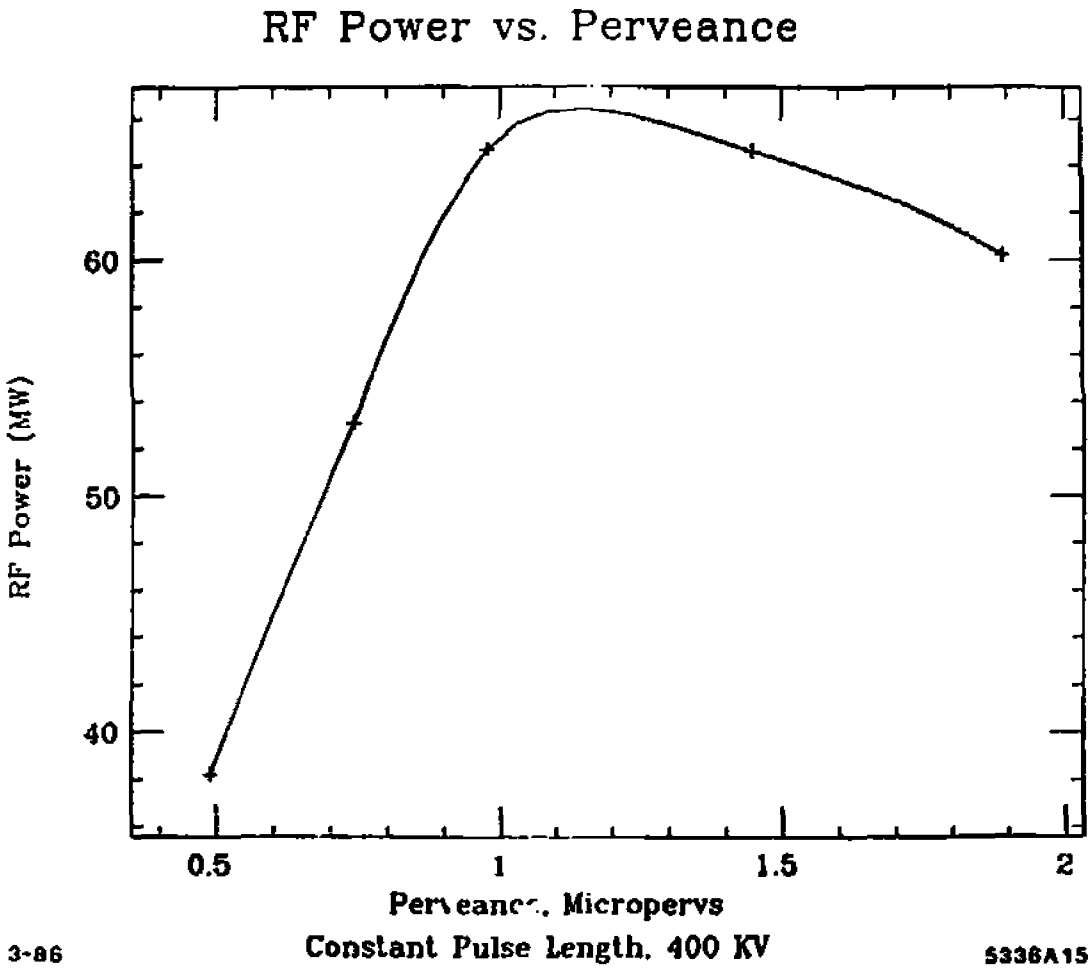
RF Power vs. Perveance
RF Power (MW)
60
50
40
0.5
1
1.5
2
Perveance, Micropervs
Constant Pulse Length, 400 KV
3-86
5336A15

FIGURE 5A

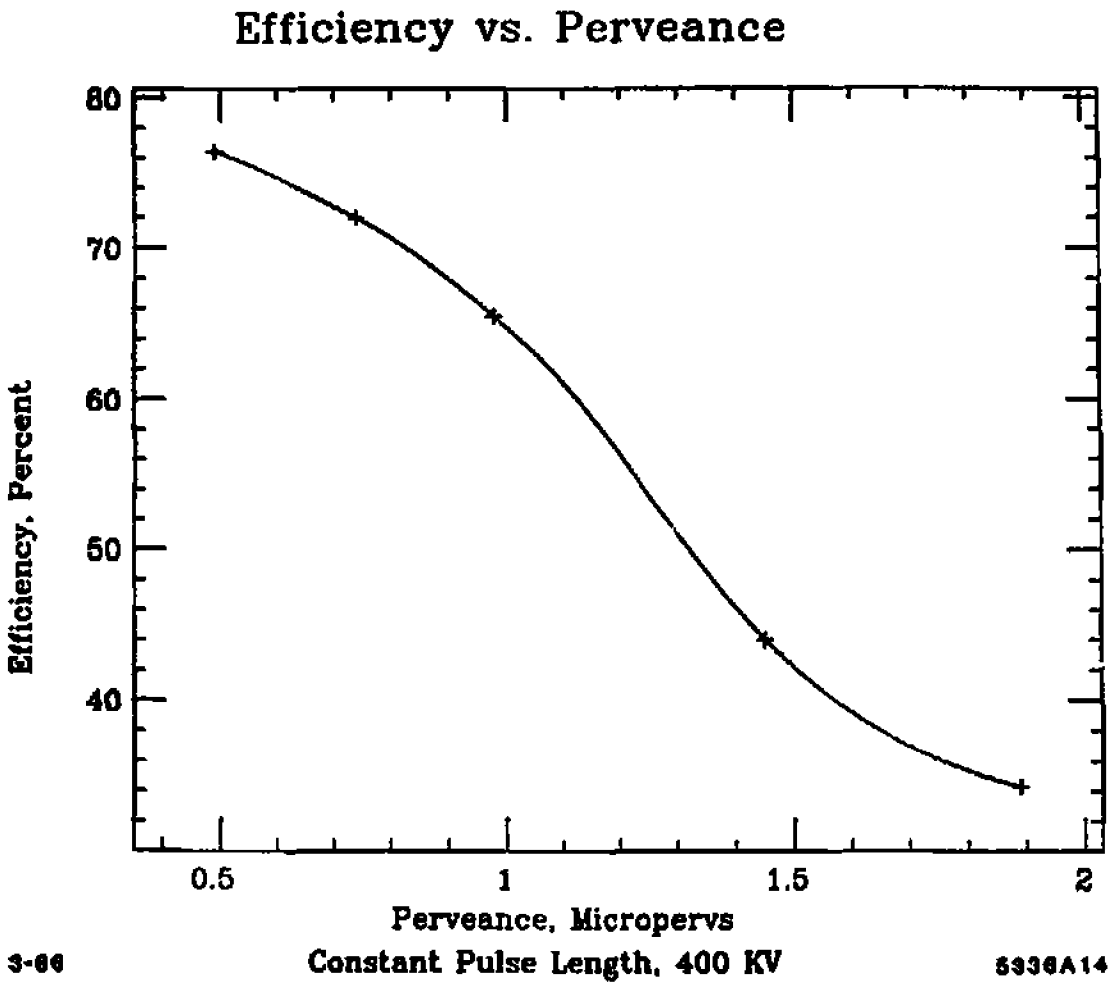
Efficiency vs. Perveance
80
70
60
50
40
Efficiency, Percent
0.5
1
1.5
2
Perveance, Micropervs
3-66
Constant Pulse Length, 400 KV
5936A14

FIGURE 5B

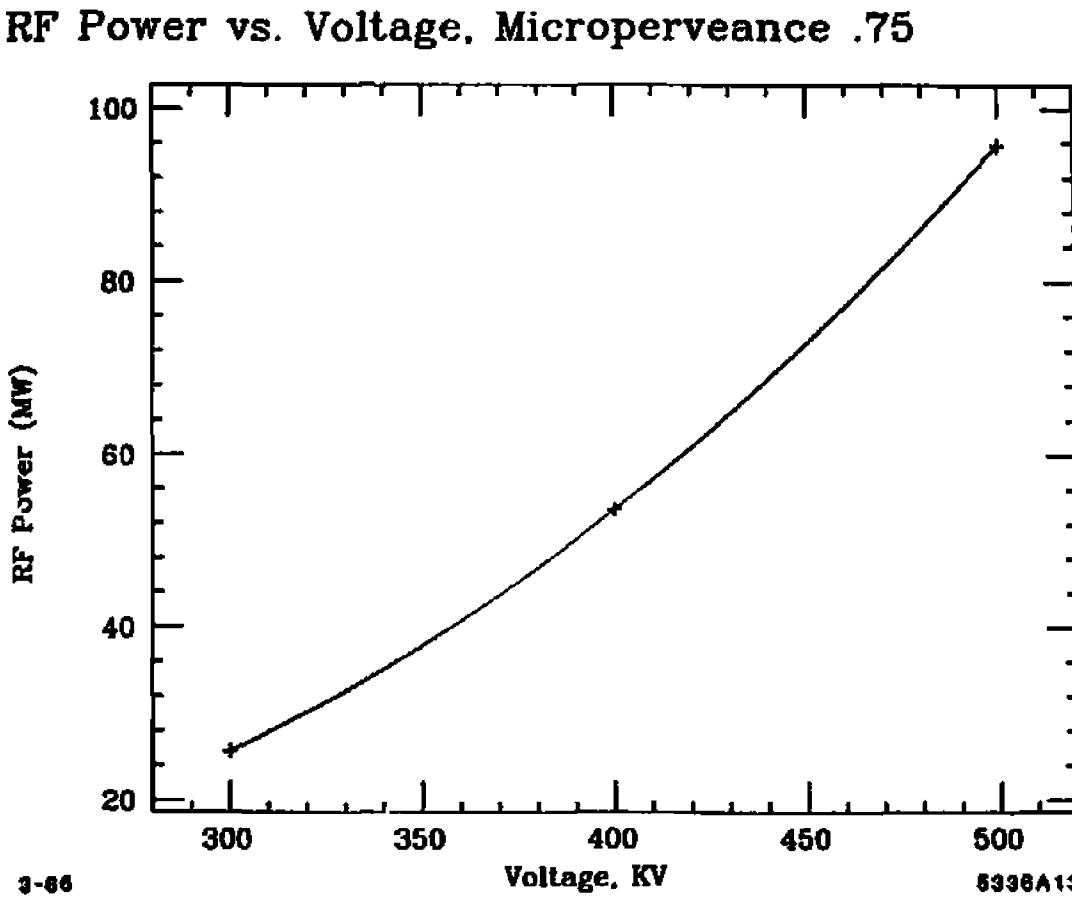
RF Power vs. Voltage, Microperveance .75
100
80
60
40
20
RF Power (MW)
300
350
400
450
500
Voltage, KV
3-66
5336A13

FIGURE 6A

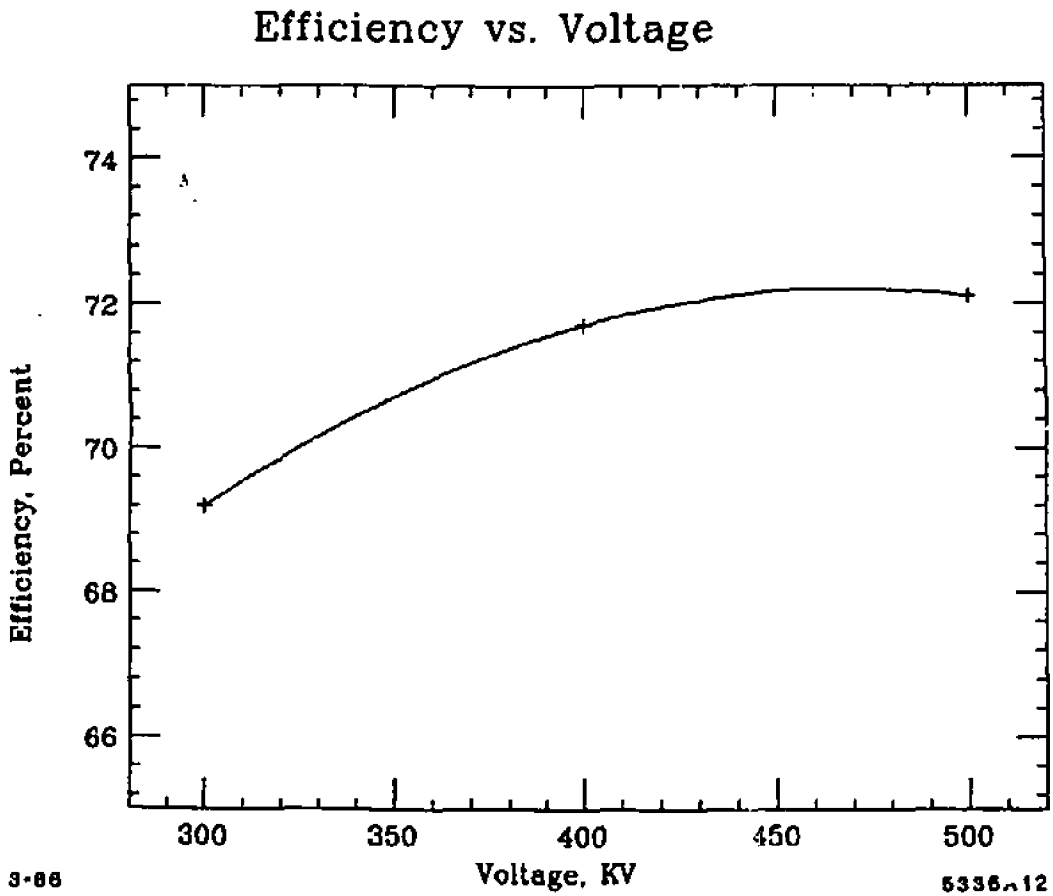
Efficiency vs. Voltage
74
72
70
68
66
Efficiency, Percent
300
350
400
450
500
Voltage, KV
3-86
5336-12

FIGURE 6B

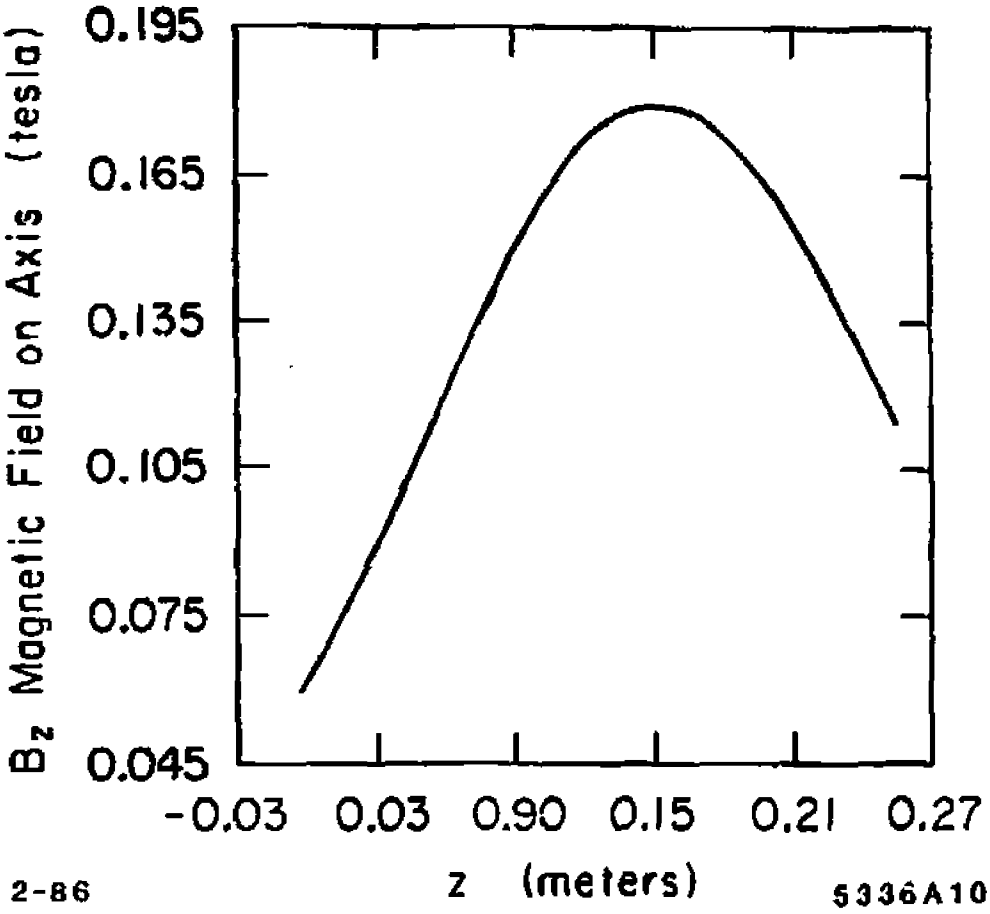
0.195
0.165
0.135
0.105
0.075
0.045
B_z Magnetic Field on Axis (tesla)
-0.03
0.03
0.90
0.15
0.21
0.27
Z (meters)
2-86
5336A10

FIGURE 7

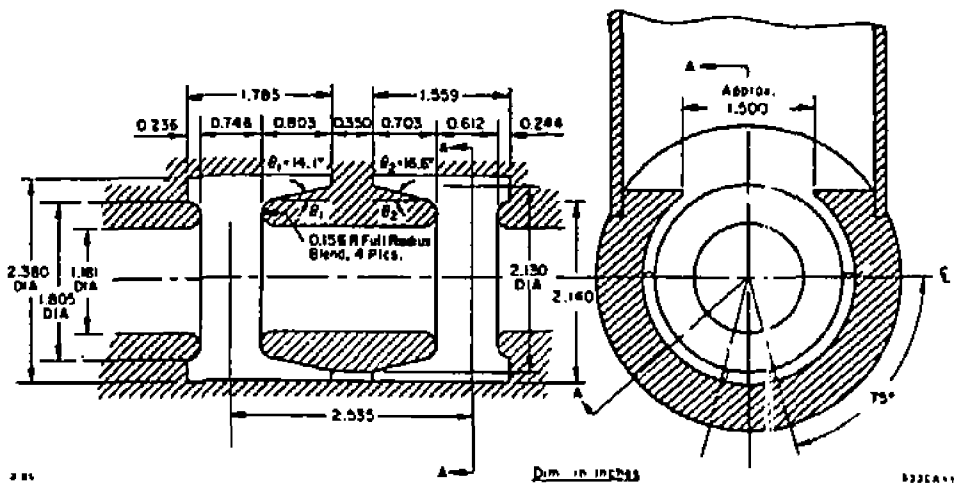
1.785
1.559
0.236
0.748
0.803
0.350
0.703
0.612
0.246
0.156 R Full Radius Blend, 4 Plcs.
2.380 DIA
1.805 DIA
1.181 DIA
2.130 DIA
2.160
2.535
1.500
75°
Dim. in inches

FIGURE 8